


RESEARCH ARTICLE

# Expression of the FGFR2c mesenchymal splicing variant in human keratinocytes inhibits differentiation and promotes invasion

Danilo Ranieri<sup>1</sup> | Benedetta Rosato<sup>1</sup> | Monica Nanni<sup>1</sup> | Francesca Belleudi<sup>1</sup> |  
Maria Rosaria Torrisi<sup>1,2</sup> 

<sup>1</sup>Laboratory affiliated to Istituto Pasteur Italia—Fondazione Cenci Bolognetti, Department of Clinical and Molecular Medicine, Sapienza University of Rome, Roma, Lazio, Italy

<sup>2</sup>S. Andrea University Hospital, Rome, Italy

## Correspondence

Prof. Maria Rosaria Torrisi and Prof. Francesca Belleudi, Laboratory affiliated to Istituto Pasteur Italia—Fondazione Cenci Bolognetti, Department of Clinical and Molecular Medicine, Sapienza University of Rome, Dip. Medicina Clinica e Molecolare, Viale Regina Elena 324, 00161 Roma, Italy.  
Email: mara.torrisi@uniroma1.it (M.R.T); francesca.belleudi@uniroma1.it (F.B)

## Funding information

MIUR and from AIRC—Associazione Italiana per la Ricerca sul Cancro, Italy, Grant number: IG 15858

The altered isoform switching of the fibroblast growth factor receptor 2 (FGFR2) and aberrant expression of the mesenchymal FGFR2c isoform in epithelial cells is involved in cancer progression. We have recently described that the ectopic expression of FGFR2c in normal human keratinocytes induces epithelial-mesenchymal transition and leads to invasiveness and anchorage-independent growth. Here, we extended our analysis to the effects of this FGFR2c forced expression on human keratinocyte differentiation and stratification. Our findings demonstrated that, differently from cells overexpressing the epithelial splicing variant FGFR2b, keratinocytes ectopically expressing FGFR2c are not able to form a monolayer and display decreased expression of early differentiation markers. This impaired ability to enter the differentiation program is related to the up-modulation of the transcription factor  $\Delta$ Np63. In addition, FGFR2c-expressing keratinocytes undergo defective stratification and invasion of the collagen matrix in 3D organotypic cultures, further suggesting their tumorigenic potential. Taken together, our results support the hypothesis that the receptor switching and the consequent appearance of the mesenchymal FGFR2c variant in the epithelial context would drive early steps of carcinogenesis, unbalancing the p63/FGFR interplay, and altering the paracrine response to the microenvironment.

## KEYWORDS

FGFR2, differentiation, invasion, human keratinocytes

## 1 | INTRODUCTION

The fibroblast growth factor receptor (FGFR) family is composed of four transmembrane receptor tyrosine kinases (FGFR1-4),

which regulate key physiological processes, such as cell proliferation, differentiation, migration and survival, in many different tissues.<sup>1,2</sup> The epithelial isoform of the FGFR2 (FGFR2b), generated by the tissue specific alternative splicing of the third

**Abbreviations:** cDNA, complementary DNA; DAB, diaminobenzidine; DEPC, diethylpyrocarbonate; DMEM, Dulbecco's modified Eagle's medium; DSG1, desmoglein-1; EMT, epithelial-mesenchymal transition; FBS, fetal bovine serum; FGF, fibroblast growth factor; FGFR, fibroblast growth factor receptor; HFs, human fibroblasts; HRP, horseradish peroxidase; Ig, immunoglobulin-like; K1, keratin 1; K10, keratin 10; pBp, pBABE-Puro; PBS, phosphate buffered saline; RT-PCR, reverse transcriptase-PCR; SD, standard deviation; SE, standard error.

This is an open access article under the terms of the Creative Commons Attribution-NonCommercial-NoDerivs License, which permits use and distribution in any medium, provided the original work is properly cited, the use is non-commercial and no modifications or adaptations are made.

© 2017 The Authors. *Molecular Carcinogenesis* Published by WileyPeriodicals, Inc.

immunoglobulin-like (Ig) loop (IgIII), is a well recognized modulator of the epidermal differentiation as well as of the skin homeostasis and repair.<sup>3-5</sup> Consistent with this role, studies from our group have demonstrated that FGFR2b expression and signaling promote keratinocyte early differentiation,<sup>6,7</sup> triggering the shift from the basal to the suprabasal layers of the epidermis. On the other hand, altered FGFR2 isoform switching and aberrant expression of the mesenchymal FGFR2c isoform in epithelial cells induces epithelial-mesenchymal transition (EMT)<sup>8,9</sup> and is involved in cancer progression.<sup>10,11</sup>

As a consequence of the initiation of a pathological cancer-associated type III EMT process driven by the ectopic expression of FGFR2c in normal human keratinocytes, we have also recently described that the mesenchymal-like morphology, actin reorganization, and modulation of EMT markers led to invasiveness and anchorage-independent growth of the cells.<sup>9</sup> These interesting observations prompted us to further investigate the behaviour of our cell model of keratinocytes, ectopically expressing the mesenchymal FGFR2c variant, during *in vitro* differentiation and stratification and in comparison with cells endogenously expressing or overexpressing by transfection the epithelial FGFR2b isoform. Through a combined application of three-dimensional (3D) organotypic cultures and molecular approaches, we found that the FGFR2c expressing keratinocytes not only underwent defective differentiation and stratification, but they were able to efficiently invade the collagen matrix, further suggesting their tumorigenic potential.

Since we have previously demonstrated that the FGFR2b overexpression is able to induce keratinocyte early differentiation also through down-modulation of the transcription factor p63,<sup>7</sup> implying the existence of a FGFR2b/p63 crosstalk balancing epithelial differentiation, we also wondered if the forced expression of the mesenchymal receptor variant would affect this crosstalk. In fact, the  $\Delta$ Np63 isoform, which is expressed in the basal cells of stratified epithelial tissues such as human skin,<sup>12</sup> is required for keratinocyte differentiation<sup>12,13</sup> and triggers EMT when transduced in normal human keratinocytes.<sup>14</sup> In addition,  $\Delta$ Np63 appears to play an oncogenic role in squamous cell carcinoma (SCC) pathogenesis and this role might involve deregulation of paracrine FGFR signaling.<sup>15</sup> Therefore, we analyzed in the stratified epidermal equivalent rafts the impact of the FGFR2c ectopical expression on p63 transcription, showing a clear up-modulation of its transcript levels, further supporting the postulated key role of the p63/FGFR interplay in keratinocyte tumor development.<sup>16</sup>

## 2 | MATERIALS AND METHODS

### 2.1 | Cells and treatments

The human keratinocyte cell line HaCaT,<sup>17</sup> stably expressing FGFR2c (pBp-FGFR2c), overexpressing FGFR2b (pBp-FGFR2b) or the empty vector (pBp) and generated as previously described,<sup>9</sup> were cultured in Dulbecco's modified Eagle's medium (DMEM), supplemented with 10% fetal bovine serum (FBS) plus antibiotics. Primary cultures of

human fibroblasts derived from healthy skin (HFs) were obtained from patients attending the Dermatology Unit of the Sant'Andrea Hospital of Rome; all patients were extensively informed and their consent for the investigation was given and collected in written form in accordance with guidelines approved by the management of the Sant'Andrea Hospital. HFs were isolated and cultured as previously described.<sup>18</sup> For growth factors stimulation, cells grown to confluence were incubated with FGF7 (Upstate Biotechnology, Lake Placid, NY) or with FGF2 (PeproTech, London, UK) 25 ng/mL for 48 h at 37°C or left untreated.

Quantitative analysis of the percentages of cells showing elongated morphology, as well as elongated morphology associated to isolated growth, was assessed by counting in pre-confluent pBp-FGFR2c samples a total of 50 cells, randomly observed in 10 microscopic fields from three different experiments. Results have been expressed as mean values.

### 2.2 | Organotypic cultures

For 3D organotypic cultures, collagen rafts were prepared adding 5 mg/mL rat tail type I collagen (Corning, Lowell, MA) to DMEM and Reconstitution buffer (8:1:1) as previously described.<sup>19</sup> A  $1 \times 10^6$  HFs were added to 2 mL of the collagen mixture in polycarbonate micron inserts (23 mm diameter, pore size 0.3  $\mu$ m; Corning) in 6-deep well plates (Corning). The mixture was left to polymerize for 30 min at 37°C. Alternatively, rafts were prepared without fibroblasts. After 24 h  $2 \times 10^5$  HaCaT pBp, pBp-FGFR2b or pBp-FGFR2c cells were seeded on the collagen gel and left to grow for a week in complete medium added in both the top and the bottom wells. Then, the organotypic cultures were lifted to the air-liquid interface and cultured for further 2 weeks in complete medium supplemented or not with FGF7 (Upstate Biotechnology) or with FGF2 (PeproTech) 25 ng/mL. Rafts were finally fixed in 10% formalin, embedded in paraffin and 4  $\mu$ m slices were stained with hematoxylin and eosin using standard procedures. Bright field images of the slices were taken with an Axiocam ICc 5 (Zeiss, Oberkochen, Germany) connected with an Axioplan 100 microscope (Zeiss). The organotypic culture thickness was measured using the Axiovision software (Zeiss) and expressed as mean  $\mu$ m  $\pm$  SD. Invasive events were counted as previously described<sup>20</sup> and expressed as mean number of events per cm  $\pm$  SD.

### 2.3 | Immunohistochemistry

Organotypic raft sections, obtained as above, were deparaffinized in xylene and re-hydrated through graded ethanols to PBS, pH 7.4. Antigen retrieval was achieved by heating sections in target retrieval solution high pH (Dako, Carpinteria, CA) for 15 min at 97°C and endogenous peroxidase activities were blocked by peroxidase blocking reagent (Dako) for 10 min at 25°C. Sections were then washed with PBS and probed with rabbit polyclonal anti-K1 (1:500 in PBS, AF 87, Covance, Princeton, NJ) for 1 h in a humidified chamber. Slides were washed extensively in PBS and detection was performed using an HRP-conjugated secondary antibody (Dako) followed by

colorimetric detection using DAB substrate chromogen (Dako) for 5 min. Sections were counterstained with hematoxylin, dehydrated with ethanol and xylene and permanently mounted under a coverslip.

## 2.4 | Immunofluorescence

HaCaT clones, grown on coverslips, were fixed with 4% paraformaldehyde in PBS for 30 min at 25°C followed by treatment with 0.1 M glycine for 20 min at 25°C and with 0.1% Triton X-100 for additional 5 min at 25°C to allow permeabilization. Cells were then incubated for 1 h at 25°C with the following primary antibodies: mouse monoclonal anti-E cadherin (1:25 in PBS; NCH-38, Dako), rabbit polyclonal anti-K1 (1:50 in PBS, AF 87, Covance), mouse monoclonal anti-DSG1 (1:20 in PBS; 27B2, Life Technologies, Carlsbad, CA). The primary antibodies were visualized using goat anti-mouse IgG-Texas Red (1:200 in PBS; Jackson ImmunoResearch Laboratories, West Grove, PA), goat anti-rabbit IgG-Texas Red (1:200 in PBS; Jackson ImmunoResearch Laboratories), goat anti-mouse IgG-Alexa Fluor 488 (1:200 in PBS; Life Technologies) for 30 min at 25°C. Nuclei were stained with DAPI (1:1000 in PBS; Sigma, Saint Louis, MO). Coverslips were finally mounted with mowiol (Sigma) for observation. Fluorescence signals were analyzed by conventional fluorescence or by scanning cells in a series of sequential sections with an ApoTome System (Zeiss) connected with an Axiovert 200 inverted microscope (Zeiss); image analysis was performed by the Axiovision software (Zeiss) and images were obtained by 3D reconstruction of the total number of the serial optical sections. Quantitative analysis of the fluorescence intensity was performed by the Axiovision software (Zeiss), analyzing 10 different fields randomly taken from three independent experiments; results are shown as means  $\pm$  SE. Organotypic raft sections were deparaffinized and blocked using 10% bovine calf serum and 0.2% Triton X-100 for 30 min at 25°C before staining as above.

## 2.5 | Western blot analysis

Cells were lysed in a buffer containing 50 mM HEPES, pH 7.5, 150 mM NaCl, 1% glycerol, 1% Triton X-100, 1.5 mM MgCl<sub>2</sub>, 5 mM EGTA, supplemented with protease inhibitors (10  $\mu$ g/mL aprotinin, 1 mM PMSF, 10  $\mu$ g/mL leupeptin), and phosphatase inhibitors (1 mM sodium orthovanadate, 20 mM sodium pyrophosphate, 0.5 M NaF). A range between 20 and 50  $\mu$ g of total protein was resolved under reducing conditions by 8% or 12% SDS-PAGE and transferred to reinforced nitrocellulose (BA-S 83, Schleider and Schuell, Keene, NH). The membranes were blocked with 5% nonfat dry milk in PBS 0.1% Tween 20 and incubated with anti-E-cadherin (NCH-38, Dako), anti-DSG1 (27B2, Life Technologies), anti-vimentin (V9, Dako) monoclonal antibodies, or with anti-K1 polyclonal antibodies (AF 87, Covance), anti-Bek polyclonal antibodies (C-17, Santa Cruz Biotechnology, CA), anti-pFGFR

(Tyr653/654) monoclonal antibody (55H2, Cell Signaling, Boston, MA), all followed by enhanced chemiluminescence detection (ECL, Amersham, Alington Heights, IL). The membranes were rehydrated and probed again with anti- $\beta$ -actin (AC-15, Sigma) or anti- $\alpha$ -tubulin (B7, Santa Cruz Biotechnology, Santa Cruz, CA) monoclonal antibodies to estimate the protein equal loading. Densitometric analysis was performed using Quantity One Program (Bio-Rad Laboratories, Hercules, CA). Results from three different experiments were normalized, expressed as fold increase respect to the control value and reported as mean values.

## 2.6 | Primers

Oligonucleotide primers necessary for target genes and the housekeeping gene were chosen utilizing the online tool Primer-BLAST<sup>21</sup> and purchased from Invitrogen (Carlsbad, CA). Primers list and characteristics are reported in Table 1. For each primer pair, we performed no-template control and no-reverse-transcriptase control (RT negative) assays, which produced negligible signals.

**TABLE 1** Primer list

Primer	Sequence
FGFR1b forward	5'-CGGGGATTAATAGCTCGGATG-3'
FGFR1b reverse	5'-GCACAGGTCTGGTACAGTGA-3'
FGFR1c forward	5'-TGGGAGCATTAAACCACACTACC-3'
FGFR1c reverse	5'-GCACCTCCATTTCCTTGTCG-3'
FGFR2b forward	5'-CGTGGAAAAGAACGGCAGTAAATA-3'
FGFR2b reverse	5'-GAACTATTTATCCCCGAGTGCTTG-3'
FGFR2c forward	5'-TGAGGACGCTGGGAATATACG-3'
FGFR2c reverse	5'-TAGTCTGGGAAGCTGTAATCTCCT-3'
FGFR3b forward	5'-TGCTGAATGCCTCCCACG-3'
FGFR3b reverse	5'-CGAGGATGGAGCGTCTGTGC-3'
FGFR3c forward	5'-CGCCCTACGCTACTGTAATA-3'
FGFR3c reverse	5'-GTGACATTGTGAAGGACAGAAC-3'
FGFR4 forward	5'-CTGTGGCCGTCAGATGCTCAA-3'
FGFR4 reverse	5'-ATGTTCTTGTGTCGGCCGATCA-3'
K10 forward	5'-GATGTGAATGTGGAAATGAATGCTG-3'
K10 reverse	5'-TGTAGTCAGTTCCTTCTCTTTTCA-3'
DSG1 forward	5'-GTGGGAGAAAAGAAAAGAACAGAGAAG-3'
DSG1 reverse	5'-CTACCACCACCAGAAAATGAACAG-3'
p63 forward	5'-CGCCGCAATAAGCAACAG-3'
p63 reverse	5'-GTAGCCTCTTACTTCTCTTCC-3'
IL-1 $\alpha$ forward	5'-GCTGAAGGAGATGCCTGAGATA-3'
IL-1 $\alpha$ reverse	5'-TTAGTGCCGTGAGTTTCCCA-3'
TCF7L1 forward	5'-CTCGTCCCACAGCAAGGC-3'
TCF7L1 reverse	5'-GAGGAGAGAACCAGTGGAGA-3'
18s forward	5'-AACCAACCCGGTCAGCCCCCT-3'
18s reverse	5'-TTCGAATGGGTCGTCGCCGC-3'

## 2.7 | RNA extraction and cDNA synthesis

Organotypic cultures were deparaffinized and RNA was extracted using the TRIzol method (Invitrogen) according to manufacturer's instructions and eluted with 0.1% diethylpyrocarbonate (DEPC)-treated water. Each sample was treated with DNAase I (Invitrogen). Total RNA concentration was quantitated by spectrophotometry; 1 µg of total RNA was used to reverse transcription using iScript™ cDNA synthesis kit (Bio-Rad) according to manufacturer's instructions.

## 2.8 | PCR amplification and real-time quantitation

Real-Time RT-PCR was performed using the iCycler Real-Time Detection System (iQ5 Bio-Rad) with optimized PCR conditions. The reaction was carried out in 96-well plate using iQ SYBR Green Supermix (Bio-Rad) adding forward and reverse primers for each gene and 1 µL of diluted template cDNA to a final reaction volume of 15 µL. All assays included a negative control and were replicated three times. The thermal cycling program was performed as described.<sup>9</sup> Real-time quantitation was performed with the help of the iCycler IQ optical system software version 3.0a (Bio-Rad), according to the manufacturer's manual. Results are reported as mean ± SE from three different experiments in triplicate.

## 2.9 | Statistical analysis

Data were statistically analyzed with unpaired two-tailed Student's *t*-test. Differences were considered significant at the level of  $P < 0.05$ . Statistical analysis was performed by using Microsoft Excel 2016 Spreadsheet Software (Microsoft® Software; Redmond, WA).

# 3 | RESULTS

## 3.1 | The forced expression of FGFR2c in human keratinocytes impairs basal layer formation

To analyze in detail the effects of the ectopic expression of the mesenchymal FGFR2c isoform on the differentiation of human keratinocytes, we used the HaCaT cell line,<sup>17</sup> widely utilized as a model of epidermal differentiation and stratification, stably transduced with pBp-FGFR2b or pBp-FGFR2c retroviral constructs or with empty pBp vector as negative control as previously described.<sup>9</sup> As expected,<sup>9</sup> FGFR2b mRNA was expressed at lower levels in all cells, testifying the endogenous expression of this epithelial isoform, but highly overexpressed only in pBp FGFR2b cells; in contrast, FGFR2c mRNA was detected in HFs, highly expressed in pBp-FGFR2c cells, but undetectable in pBp controls or pBp-FGFR2b cells (Supplementary Figure S1A). In addition, the forced expression of either FGFR2b or FGFR2c isoform did not affect the transcript levels of the other FGFRs and their variants (FGFR1b and c, FGFR3b and c, FGFR4) (Supplementary Figure S1B).

Since our recent observations on HaCaT keratinocytes expressing FGFR2c demonstrated that these cells display a greater tendency to

form disorganized colonies compared to HaCaT control or HaCaT cells overexpressing the epithelial splice variant FGFR2b,<sup>9</sup> first we investigated the ability to reach confluence and to form a monolayer of the stable clones left grown at different levels of cell density. Low magnification phase contrast analysis confirmed that, while pre-confluent pBp and pBp-FGFR2b cultures were closely packed and characterized by the typical polygonal shape of epithelial cells (Figure 1A, upper panels), pBp-FGFR2c cultures contained single elongated elements reminiscent of mesenchymal cells (Figure 1A, upper panels: arrows and detail on the right panel). Quantitative evaluation, performed as described in Section 2, revealed that the percentage of elongated cells in pre-confluent HaCaT pBp-FGFR2c cultures was variable (ranging from 21% to 30%), with approximately 46% of these spindle-shaped cells detached from the colonies and displaying an isolated growth tendency. At confluence, both HaCaT pBp and HaCaT pBp-FGFR2b clones appeared to form a continuous monolayer (Figure 1A, lower panels), whereas pBp-FGFR2c cultures were not able to reach a well-organized monolayer as a consequence of the isolated pattern of growth (Figure 1A, lower panels, arrows). Thus, the mesenchymal phenotype driven by FGFR2c expression appears to impair the ability of keratinocytes to form a basal layer.

The contiguity of the keratinocyte basal layer is guaranteed by cadherin-based junctions and E-cadherin is a key component of the adherens junctions responsible for epithelial differentiation [reviewed in Ref. 22]. We have recently reported that the ectopic expression of FGFR2c drives the E-cadherin down-regulation occurring during EMT.<sup>9</sup> To understand if the less packed organization observed in pBp-FGFR2c cultures could be attributed to adherens junctions disorganization, the expression levels of E-cadherin were evaluated by immunofluorescence analysis of confluent cultures as above. Results demonstrated that, in both pBp and pBp-FGFR2b cells, the signal for E-cadherin was clearly visible at the plasma membrane and at the cell-cell contacts (Figure 1B), while it became quite undetectable at the cell surface in pBp-FGFR2c cultures (Figure 1B). The presence of E-cadherin-positive intracellular dots in the clones expressing FGFR2c (Figure 1B, arrowheads) suggested disassembling of the junctions and E-cadherin internalization and possible degradation: in fact, although the loss of E-cadherin can be often due to a transcriptional repression, massive internalization, and degradation of this epithelial marker could also contribute to its down-regulation.<sup>23</sup> Quantitative analysis of the fluorescence intensity performed as described in Section 2 confirmed that E-cadherin staining was significantly reduced in HaCaT pBp-FGFR2c cells compared to either pBp-FGFR2b or control cells (Figure 1B). The down-regulation of E-cadherin in cells stably expressing FGFR2c and left to grow until confluence was confirmed by Western blot analysis. In agreement with our previous findings,<sup>9</sup> a reduction of the band corresponding to the epithelial marker is visible only in HaCaT FGFR2c clones, while FGFR2b cultures maintained E-cadherin levels comparable to control cells (Figure 1C, left panel). Moreover, consistent with the role of FGFR2c in the acquisition of the mesenchymal phenotype during EMT,<sup>9</sup> the down-regulation of E-cadherin was accompanied by the appearance of the mesenchymal marker vimentin in FGFR2c expressing cells (Figure 1C, right panel).

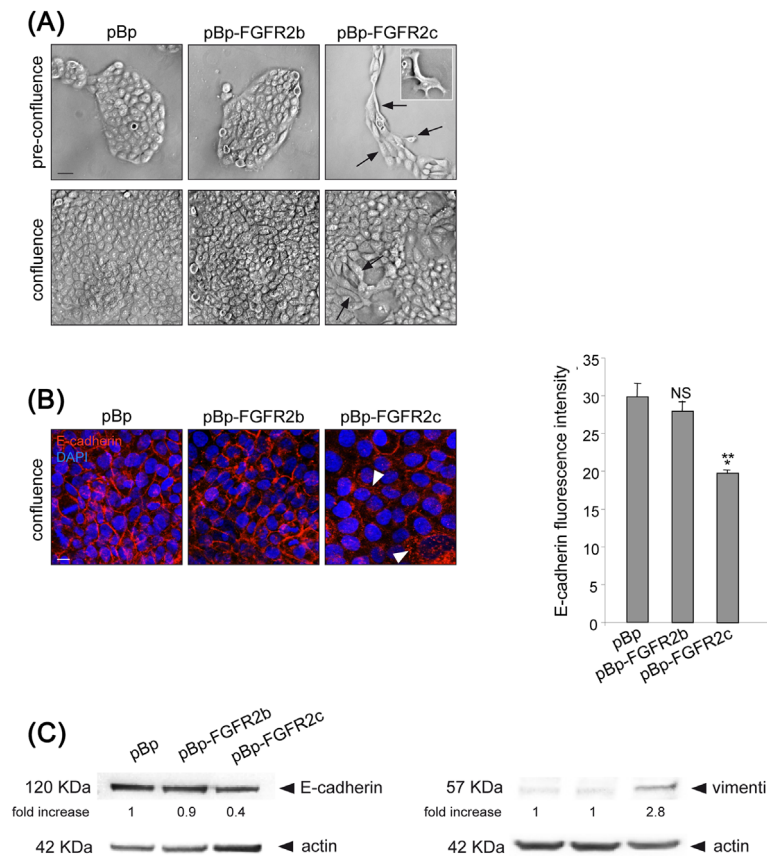


**FIGURE 1** The forced expression of FGFR2c affects basal layer organization. (A) HaCaT cells, stably transduced with pBp-FGFR2b or pBp-FGFR2c constructs or with the empty pBp retroviral vector as control, were left to grow to pre-confluence or confluence. Phase contrast microscopy shows that pre-confluent pBp-FGFR2b and control pBp cells are closely packed and display the typical epithelial morphology (upper panels), while pBp-FGFR2c cultures contain isolated and elongated mesenchymal-like cells, located at the periphery of the colonies (upper panels, arrows and detail in the right panel). When confluent, both pBp and pBp-FGFR2b clones form a continuous monolayer (lower panels), while pBp-FGFR2c cultures do not organize a compact monolayer (lower panels, arrows). Images are representative of three independent experiments. Bar: 25  $\mu$ m. (B) Immunofluorescence analysis was performed in confluent cell cultures and nuclei were stained with DAPI. In both pBp and pBp-FGFR2b cells the E-cadherin signal is evident at the plasma membrane and at the cell-cell contacts, while in pBp-FGFR2c cultures the staining appears very low and mostly localized in intracellular dots (arrowheads). Quantitative analysis of the fluorescence intensity performed as described in Section 2 shows that the total E-cadherin signal is significantly reduced in pBp-FGFR2c compared to either pBp-FGFR2b or control cells. Results are expressed as mean values  $\pm$  SE from three independent experiments. Student *t* test was performed and significance levels have been defined as  $p < 0.05$ : NS vs pBp cells; \* $p < 0.001$  vs pBp cells; \*\* $< 0.01$  vs pBp-FGFR2b cells. Bar: 10  $\mu$ m. (C) Western blot analysis, performed in confluent cultures, shows a reduction of the band corresponding to the epithelial marker E-cadherin and the appearance of the band corresponding to the mesenchymal marker vimentin in pBp-FGFR2c clones, while the protein levels are comparable in pBp-FGFR2b and pBp cells. The equal loading was assessed using anti- $\beta$  actin antibody. For densitometric analysis results are expressed as mean values from three independent experiments

The equal loading was assessed with anti- $\beta$  actin antibody and densitometric analysis was performed as described in Section 2.

### 3.2 | FGFR2c expression inhibits early differentiation

While we have previously shown the role of FGFR2b expression and signaling in the induction of the early differentiation of human keratinocytes,<sup>6,7</sup> the effect of the forced expression of the FGFR2c mesenchymal isoform on this process remains still to be elucidated. Therefore, with the aim to analyze the capacity to advance in the early differentiation program of the HaCaT FGFR2c versus HaCaT FGFR2b clones we first evaluated the

process monitoring the appearance of the early differentiation marker keratin 1 (K1). Cells were left to grow in complete medium until post-confluence and the expression of K1 was assessed by quantitative immunofluorescence analysis. The results showed that, similarly to that obtained in HaCaT non transfected cells,<sup>24</sup> in pBp control cultures the K1 cytosolic signal was clearly visible in suprabasal cells (Figure 2A, single asterisks), while the basal cells appeared unstained (Figure 2A, double asterisk). In addition, consistently with our previous data showing that FGFR2b overexpression increases the K1 protein expression,<sup>6,7</sup> pBp-FGFR2b cells were mostly positive for K1 and the signal intensity significantly increased compared to control cells (Figure 2A). In

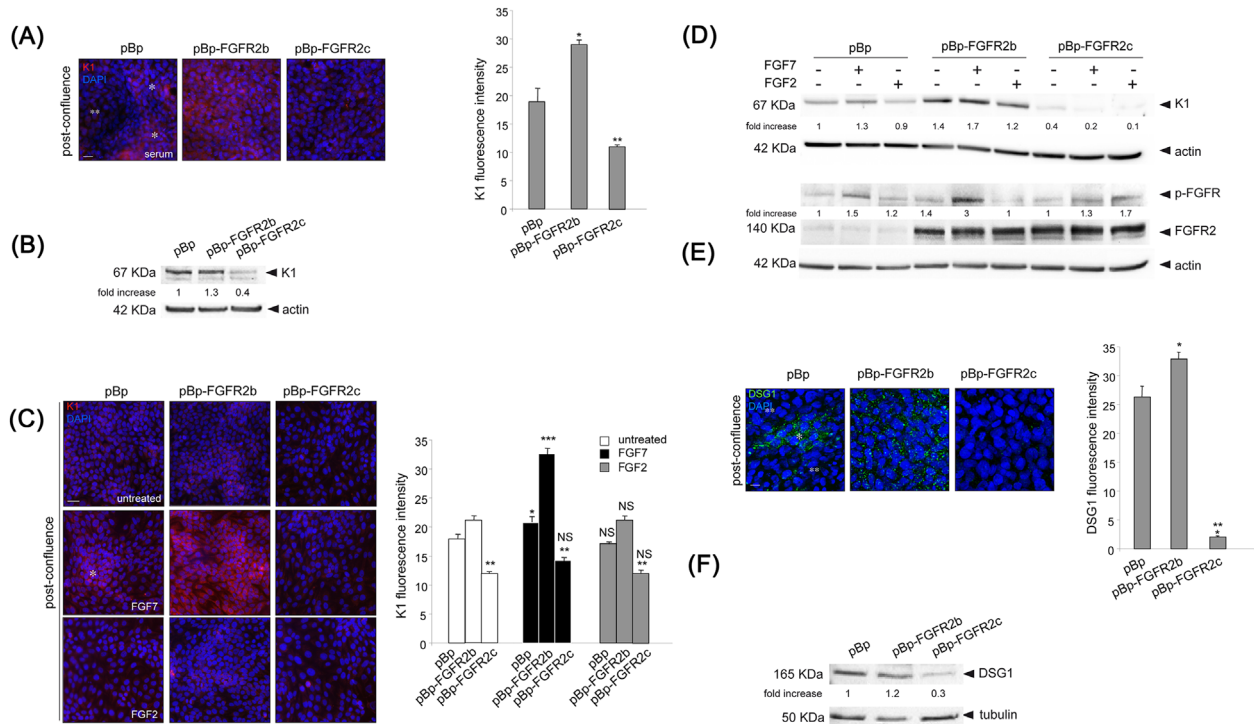


**FIGURE 2** FGFR2c expression and ligand-dependent activation inhibit keratinocyte differentiation. (A) HaCaT pBp, pBp-FGFR2b, or pBp-FGFR2c clones were grown to post-confluence. Quantitative immunofluorescence analysis shows that the K1 signal is highly reduced in pBp-FGFR2c cultures, while the fluorescence intensity of pBp-FGFR2b cells is significantly increased compared to control cells. In pBp cultures the K1 staining is visible in the suprabasal cells (single asterisks) and undetectable on the basal layer (double asterisk), while pBp-FGFR2b cells are mostly positive for K1 staining. Results are expressed as mean values  $\pm$  SE from three independent experiments. Student *t* test was performed and significance levels have been defined as  $p < 0.05$ ; \* $p < 0.001$  and \*\* $p < 0.05$  vs the corresponding pBp cells. Bar: 20  $\mu$ m (B) Western blot analysis performed in post-confluent HaCaT clones shows that the levels of the band corresponding to K1 marker are slightly increased in pBp-FGFR2b clones, but clearly decreased in FGFR2c expressing cells compared to pBp cells. The equal loading and the densitometric analysis were assessed as above. (C) HaCaT clones were grown in complete medium until confluence and then treated for 48 h with FGF7, with FGF2 or left untreated. Immunofluorescence analysis shows that, after FGF7 stimulation, the K1 staining is increased in pBp suprabasal cells (asterisk), and further enhanced and more uniformly distributed in pBp-FGFR2b cultures, while no significant effects are detectable in pBp-FGFR2c cultures compared to the untreated cells. In contrast, in all cultures, FGF2 stimulation does not affect K1 expression. Results are expressed as mean values  $\pm$  SE from three independent experiments. Student *t* test was performed and significance levels have been defined as  $p < 0.05$ : NS, \* $p < 0.05$  and \*\*\* $p < 0.001$  vs the corresponding untreated cells, \*\* $p < 0.001$  vs the corresponding pBp cells. Bar: 20  $\mu$ m (D) Western blot analysis of the HaCaT clones stimulated with the growth factors as in C shows that, while the levels of K1 expression in both pBp and pBp-FGFR2b cells are increased in response to FGF7, FGF2 treatment is not able to modulate the protein levels. Parallel evaluation of the receptor tyrosine phosphorylation, performed using anti-Bek polyclonal antibodies, and anti-pFGFR (Tyr653/654) monoclonal antibody, shows that the thick bands, corresponding to the receptor molecular weight in pBp-FGFR2b and pBp-FGFR2c, appear more phosphorylated after treatment with the specific growth factor FGF7 and FGF2, respectively. The thin band visible in pBp cells, corresponding to the endogenous expression of the FGFR2b isoform, is phosphorylated upon FGF7 stimulation. The equal loading was assessed with anti- $\beta$  actin antibody and densitometric analysis was performed as above. (E) Immunofluorescence analysis performed in post-confluent HaCaT clones shows that, in pBp cultures, the punctate staining of DSG1, undetectable on the basal layer (double asterisks), becomes evident in the suprabasal differentiated cells (single asterisk). DSG1 signal is homogeneously distributed and significantly increased in pBp FGFR2b clones, but is almost undetectable in pBp-FGFR2c cultures compared to controls. Results are expressed as mean values  $\pm$  SE from three independent experiments. Student *t* test was performed and significance levels have been defined as  $p < 0.05$ : \* $p < 0.05$  vs pBp cells and \*\* $p < 0.01$  vs pBp-FGFR2b cells. Bar: 10  $\mu$ m (F) Western blot analysis, performed in post-confluent cultures shows a clear decrease of the band corresponding to DSG1 in pBp-FGFR2c clones, while the protein levels are slightly increased in FGFR2b overexpressing cells compared to controls. The equal loading was assessed using anti-tubulin antibody. Densitometric analysis was performed as above

contrast, in pBp-FGFR2c cultures, the K1 staining appeared very low and significantly reduced (Figure 2A). This opposite modulation of the K1 marker, induced by the differential expression of FGFR2b or FGFR2c, was also investigated by Western blot analysis. The band at the molecular weight corresponding to K1 appeared slightly increased in HaCaT pBp-FGFR2b, but strongly

decreased in HaCaT pBp-FGFR2c cells compared to controls (Figure 2B). The equal loading was assessed with anti- $\beta$  actin antibody and densitometric analysis was performed as above. These results suggested that, while stable FGFR2b overexpression enhances the keratinocyte early differentiation as expected,<sup>6,7</sup> the FGFR2c ectopic expression inhibits it.

The alternative splicing of the FGFRs is known to determine the ligand specificity and our cell models of HaCaT pBp-FGFR2b or FGFR2c cells are specifically activated by their corresponding ligands.<sup>9</sup> Therefore, in order to assess the possible impact of FGFR2b or 2c signaling on keratinocyte differentiation and K1 expression, cells were left to grow in complete medium up to confluence and then treated for the following 48 h with FGF7, the specific ligand of FGFR2b, or with FGF2, which does not bind to FGFR2b, but it is able to activate other FGFRs including FGFR2c, or left untreated. Quantitative immunofluorescence analysis performed as described above showed that, upon FGF7 stimulation, the K1 staining appeared slightly increased in pBp suprabasal cells (Figure 2C, middle left panel, asterisk), and further enhanced and more uniformly distributed in pBp-FGFR2b cultures (Figure 2C, middle central panel), while no significant effect was detected in pBp-FGFR2c cultures (Figure 2C, middle right panel) compared to the untreated corresponding cells (Figure 2C, upper panels). In all cultures FGF2 stimulation was not able to alter K1 expression (Figure 2C, lower panels). These observations were also confirmed by Western blot analysis: while treatment with FGF7 induced an increase in the levels of K1 expression in both pBp and pBp-FGFR2b cells, FGF2 stimulation was not able to modulate it (Figure 2D). The higher K1 protein content in pBp-FGFR2b untreated cultures respect to the corresponding unstimulated pBp cells can be ascribed to the already acquired early differentiation of the FGFR2b clones during their growth in complete medium up to confluence. The equal loading was assessed with anti- $\beta$  actin antibody and densitometric analysis was performed as above. These results suggest that the stable and long-term forced expression of FGFR2c in keratinocyte cultures not only compromise the epithelial cell morphology and growth mode,<sup>9</sup> but also impairs the differentiation. Parallel evaluation of the tyrosine phosphorylation state of the receptors was also performed using anti-Bek polyclonal antibodies, which recognize the intracellular portion of the FGFR2 but do not discriminate between the two splicing variants, and anti-pFGFR (Tyr653/654) monoclonal antibody. The 140 KDa band, corresponding to the receptor molecular weight, was clearly visible in the pBp-FGFR2b and pBp-FGFR2c clones (Figure 2D), appearing more phosphorylated after treatment with the specific growth factor, FGF7 and FGF2, respectively. A thin band was also visible in pBp cells, corresponding to the endogenous expression of the FGFR2b isoform, and phosphorylated upon FGF7 stimulation. These observations demonstrate activation of the receptors upon treatments with the ligands, although not directly related to the positive or negative effect on the differentiative process.

To further confirm the opposite effect on keratinocyte differentiation exerted by the expression of FGFR2b or 2c isoforms, we analyzed by immunofluorescence and biochemical approaches their impact on Desmoglein-1 (DSG1), a desmosomal component expressed from the suprabasal layers [reviewed in Ref. 22] and directly involved in the initiation of early differentiation.<sup>25,26</sup> Results clearly showed that, in pBp cells, DSG1 staining, which appeared punctate and mainly distributed along the cell-cell contacts, was undetectable on the basal layer (Figure 2E, double asterisks) and became evident in the suprabasal differentiated cells (Figure 2E, single asterisk). In contrast,

in pBp-FGFR2c cultures, the DSG1 signal was almost undetectable, while the staining in pBp FGFR2b cultures appeared enhanced and homogeneously distributed compared to the pBp cells (Figure 2E). Quantitative immunofluorescence analysis performed on the 3D reconstruction of the total series of optical sections, as described in Section 2, revealed that the overall DSG1 signal was highly reduced in FGFR2c cultures and significantly increased in pBp-FGFR2b cultures compared to control pBp cells (Figure 2E). The down-regulation of DSG1 induced by FGFR2c expression was also confirmed by Western blot analysis, which showed a clear reduction of the band corresponding to DSG1 in pBp-FGFR2c compared to pBp-FGFR2b and control cells (Figure 2F). The equal loading was assessed with anti-tubulin antibody and densitometric analysis was performed as described in Section 2. Taken together, our results indicate that the ectopic expression of FGFR2c, which is known to drive EMT in keratinocytes,<sup>9</sup> is also able to alter their ability to form a basal layer and to enter the early differentiation program.

### 3.3 | FGFR2c-expressing keratinocytes undergo defective stratification and invasion of the collagen matrix in 3D organotypic cultures

Epidermal keratinocytes are able to stratify in 3D organotypic skin-equivalent cultures when seeded on a collagen matrix and exposed to the air-liquid interface.<sup>27</sup> This *in vitro* model system is known to reproduce the differentiation steps occurring *in vivo* responsible for the physiological epithelial turnover. In addition, this raft culture approach allows to study the behavior of the keratinocytes in pathological conditions, such as those induced by viral infection or cell transformation.<sup>19,27-29</sup> Therefore, to analyze the possible altered capacity of the FGFR2c keratinocytes to stratify in 3D organotypic cultures, we engineered collagen gel matrices enriched with normal human dermal fibroblasts and we seeded the pBp-FGFR2c, pBp-FGFR2b, or pBp HaCaT clones on top of the rafts as described in Section 2. The organotypic skin cultures were then fixed at the 14 days time point after the air-lift and embedded in paraffin before sectioning and staining with hematoxylin and eosin. The histological observations and random image acquisition revealed a clear impairment of stratification in 3D FGFR2c cultures compared to the FGFR2b and control skin equivalents (Figure 3A). Interestingly, close inspection at higher magnification of the keratinocyte orientation and polarity into the overlapping layers showed that, differently from FGFR2b and control rafts, the FGFR2c cells were characterized by an elongated morphology and flattened horizontal orientation of the nuclei (Figure 3A, details on the panels). The thickness of the rafts, measured by an image analysis software and expressed as  $\mu\text{m}$  mean  $\pm$  SD, confirmed the morphological observations (Figure 3D), indicating the defective stratification of FGFR2c clones.

Immunohistochemical and immunofluorescence analysis of skin equivalents demonstrated that the observed impairment of the stratification in FGFR2c cultures was accompanied by defective differentiation. In fact, staining of K1 (Figures 3B and 3C) and DSG1 (Figure 3C), that appeared increased in FGFR2b rafts (Figures 3B and

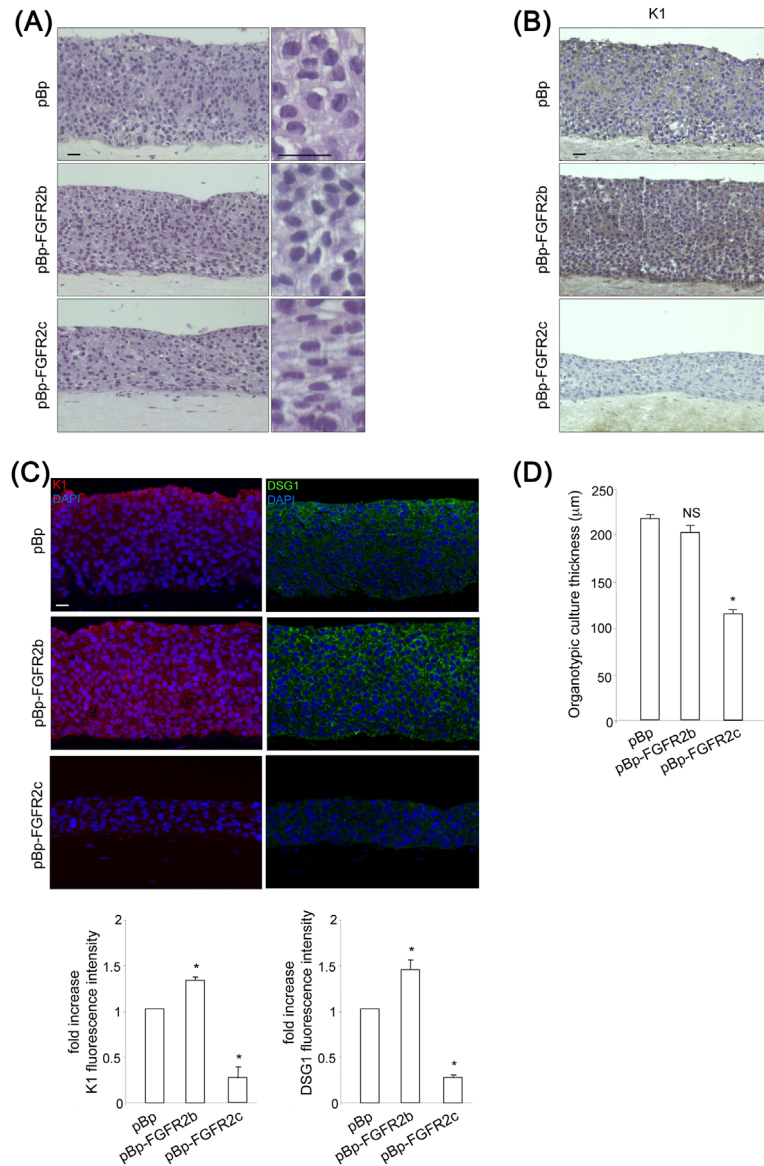


**FIGURE 3** FGFR2c expression impairs epidermal stratification and inhibits epidermal early differentiation. Organotypic skin equivalents of HaCaT pBp, pBp-FGFR2b, and pBp-FGFR2c clones were prepared as reported in Section 2. Briefly, clones were seeded on the top of HF-containing collagen gel matrices and raft cultures were fixed at 14 days after the air-lift and embedded in paraffin before sectioning and staining with hematoxylin and eosin. (A) FGFR2c cultures show impairment of stratification compared to the FGFR2b and control skin equivalents. Observation at higher magnification reveals that the single FGFR2c cells into the overlapping layers appear elongated and with flattened nuclei, while FGFR2b and control cells appear polygonal shaped (details on the right). Bars: 25 μm (B and C) Immunohistochemical (B) and quantitative immunofluorescence (C) analysis shows that, while in pBp-FGFR2b rafts K1 and DSG1 staining are increased and, differently from that observed in controls, they are already detectable in the basal layer, both signals appear strongly decreased in FGFR2c rafts. Quantitative analysis of the fluorescence intensity was performed as above and expressed as fold increase respect to pBp values. Student *t* test was performed and significance levels have been defined as  $p < 0.05$ : \* $p < 0.0001$  vs the corresponding pBp rafts. Bars: 25 μm (D) Quantitative analysis of the raft thickness was expressed as μm mean ± SD from three independent experiments. Student *t* test was performed and significance levels have been defined as  $p < 0.05$ : NS and \* $p < 0.001$  vs the corresponding pBp rafts

3C, central panels) compared to controls (Figures 3B and 3C, upper panels), were strongly decreased in FGFR2c cultures (Figures 3B and 3C, lower panels). Quantitative analysis of the fluorescence intensity confirmed the opposite trend of K1 and DSG1 expression in FGFR2b and FGFR2c rafts (Figure 3C). In addition, while in control skin equivalents these two early differentiation markers became evident

starting from the suprabasal layers (Figure 3C, upper panels), as expected,<sup>22</sup> in FGFR2b rafts the markers were already detectable in the basal layer (Figure 3C, central panels), confirming the precocious onset of the early differentiation program. Thus, since the keratinocyte stratification is consequent to their capability to correctly undergo differentiation, our results indicate that the



ectopic and prolonged expression of FGFR2c prevents keratinocytes from entering the early differentiation program and leads to a compromised stratification of the raft.

Because it is well known that defective epidermal stratification might be consequent to the molecular imbalance in the expression of the transcription factor p63 (mainly in its isoform DNp63),<sup>12,13</sup> we performed Real-time RT-PCR analysis on the organotypic cultures obtained using fibroblast-enriched gels and left growing for 14 days after the air-lift as above. First, we checked the transcript levels of both receptor isoforms and we found high levels of FGFR2b and FGFR2c only in the rafts composed of the corresponding FGFR2b or FGFR2c

clones (Figures 4A and 4B). Since the FGFR2c mRNA expression found in FGFR2b rafts (Figure 4B) could be attributed only to the fibroblasts present in the gels, in order to test this hypothesis we performed a parallel analysis of the FGFR2c expression in the rafts obtained using gel matrix devoid of fibroblasts, showing no expression of the mesenchymal receptor isoform in the absence of fibroblasts (Supplementary Figure S2), and confirming the fibroblastic origin of the FGFR2c mRNA detected in pBp and pBp-FGFR2b rafts (Figure 4B). To further validate, at molecular level, the results of inhibition of differentiation of the FGFR2c rafts, we analyzed the expression of the keratin 10 (K10) or DSG1 early differentiation markers, which

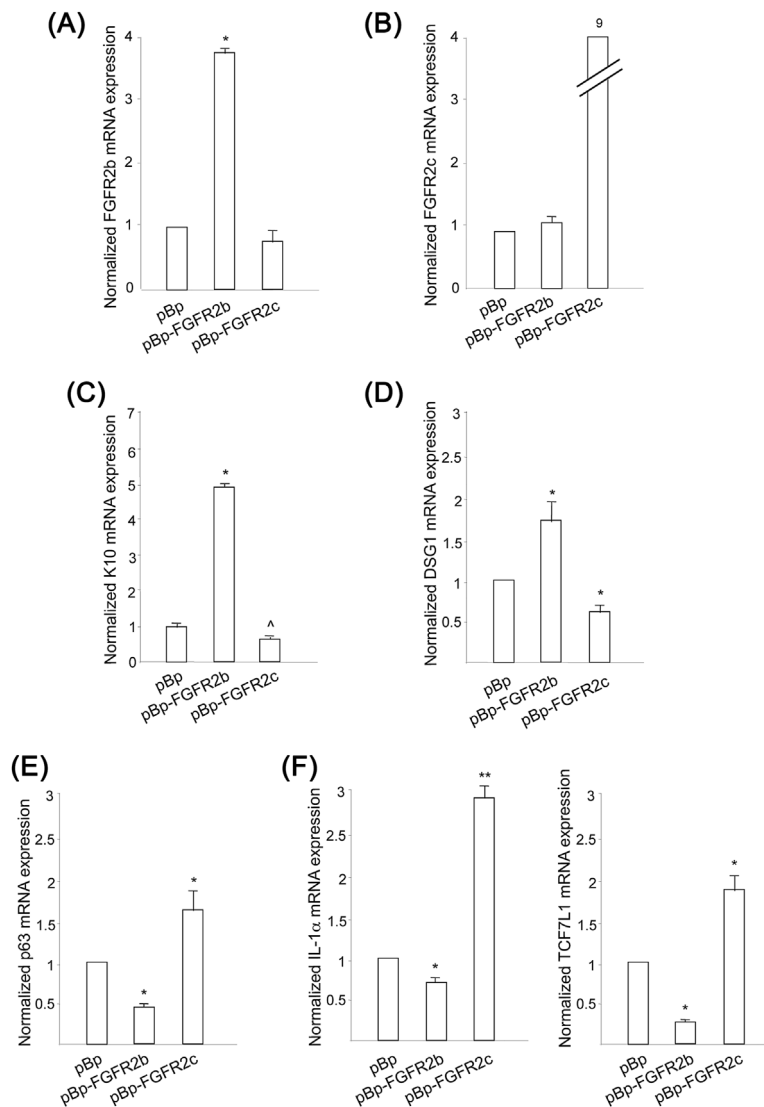


**FIGURE 4** The mRNA expression of p63 is modulated in the organotypic FGFR2b or FGFR2c rafts. Real-time RT-PCR analysis was performed in organotypic skin equivalents of HaCaT clones prepared as reported above. (A and B) High levels of FGFR2b (A) and FGFR2c (B) transcripts are detected in the rafts composed of the corresponding pBp-FGFR2b or pBp-FGFR2c clones. While the FGFR2b mRNA in cell other than pBp-FGFR2b corresponds to endogenous receptors, the FGFR2c mRNA expression in the rafts is attributable to the presence of fibroblasts in the dermal-equivalent gels. (C-E) mRNA expression of K10 and DSG1 early differentiation markers are highly down-modulated in FGFR2c rafts and up-modulated in FGFR2b cultures compared to the pBp controls (C and D), whereas mRNA expression of p63 (E) and of the p63 target genes IL-1 $\alpha$  and TCF7L1 (F) display an opposite trend (E and F). Results are expressed as mean values  $\pm$  SE from three independent experiments. Student t test was performed and significance levels have been defined as  $p < 0.05$ : (A) \* $p < 0.001$  vs the corresponding pBp rafts, (C) \* $p < 0.0005$  and <sup>^</sup> $p < 0.05$  vs the corresponding pBp rafts; D, E, F) \* $p < 0.05$  vs the corresponding pBp rafts

appeared clearly suppressed compared to the pBp, while in pBp-FGFR2b cultures they appeared strongly and significantly increased (Figures 4C and 4D). Finally, the expression levels of p63, which is down-modulated during the shift from basal to suprabasal layers in stratified epithelial tissues<sup>12</sup> and in response to FGFR2b activation by its ligand FGF7,<sup>7</sup> appeared decreased in pBp-FGFR2b rafts, but clearly increased in pBp-FGFR2c organotypic cultures (Figure 4E), in agreement with the inhibition of the early differentiation and the defective stratification of p63. Since two target genes of p63 have been identified in normal human keratinocytes<sup>30</sup>: interleukin-1 $\alpha$  (IL-1 $\alpha$ ), which is involved in the paracrine FGF7/FGFR2b crosstalk, and TCF7L1, a downstream component the Wnt signaling pathway, which appears to function in maintaining the undifferentiated state of the basal keratinocytes, we have checked their expression in the rafts. Our results demonstrated that, consistent with the observed p63 modulation (Figure 4E), the expression levels of both IL-1 $\alpha$  and TCF7L1 were clearly up-regulated in pBp-FGFR2c skin equivalents and significantly decreased in pBp-FGFR2b rafts (Figure 4F) compared to pBp controls.

3D organotypic cultures represent also a powerful model system to analyze the invasive potential of transformed epithelial cells into the collagen matrix.<sup>29</sup> Since we have shown that the mesenchymal-like morphology and actin reorganization acquired by the FGFR2c expressing keratinocytes correspond to invasiveness and anchorage-independent growth ability of the cells,<sup>9</sup> we wondered if it would be possible to observe invasive events in rafts of FGFR2c expressing cells compared to FGFR2b and control clones. The histological observations of the organotypic sections revealed the irregular shape of the skin equivalent basal layer in FGFR2c rafts, showing frequent features of matrix invasion (Figure 5A, left panels), which

were highly induced by FGF2 stimulation (Figure 5A, right panels). The quantitative evaluation of the invasive events, manually counted as described<sup>20</sup> and shown as mean number per cm  $\pm$  SD, clearly revealed that, while FGFR2b and control clones were not capable to invade the matrix, FGFR2c expressing cells were characterized by a clear invasive potential which can be further promoted by receptor activation following binding with its specific ligand FGF2 (Figure 5B). Because it has been demonstrated that, in organotypic cultures, the matrix remodeling function of the fibroblasts inside the collagen gel is essential for the invasion of the epithelial cells,<sup>31</sup> to further validate our observations we engineered our rafts using collagen gel matrices without addition of fibroblasts. Again the histological examination and measurement of the thickness showed the defective stratification of FGFR2c clones (Supplementary Figures S3A and S3B). However, the absence of fibroblasts did not allow FGFR2c clones to invade the matrix (Supplementary Figure S3C).

## 4 | DISCUSSION

Deregulation of the FGF/FGFR axis is well known to play oncogenic roles in a number of tissue contexts; however, it has been also demonstrated that the FGFR activation may lead to an opposite tumor suppressive outcome.<sup>32,33</sup> This assumption appears particularly true for FGFR2 in human carcinomas, where the epithelial isoform FGFR2b/KGFR is down-regulated in several tumors,<sup>1,32</sup> while out-of-context expression of the mesenchymal variant FGFR2c has been frequently detected.<sup>1,32,33</sup> In agreement with this opposite expression profiles, FGFR2b is able to exert a tumor suppressive role in vitro and in vivo,<sup>34,35</sup> whereas FGFR2c appears to trigger the early steps of

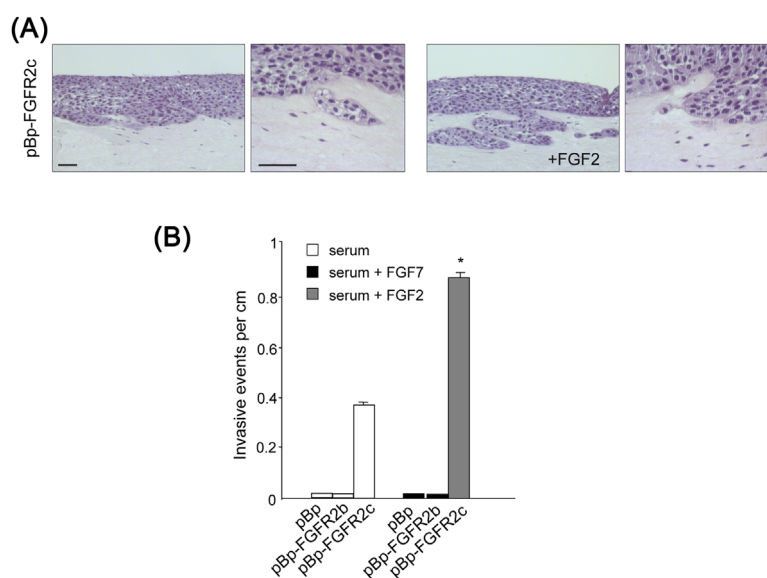


**FIGURE 5** FGFR2c expression and signaling promote invasion. Organotypic skin equivalents of HaCaT clones prepared as reported above were grown in complete medium with or without the addition of FGF7 or FGF2. Rafts were then embedded, sectioned and stained as reported above. (A) FGFR2c organotypic cultures display an irregular shape of the basal layer and frequent features of matrix invasion, which are highly induced upon FGF2 stimulation. Bar: 50  $\mu$ m. (B) The invasive events, visible only in FGFR2c cultures and only after addition of FGF2, but not FGF7, were manually counted and shown as mean number per cm  $\pm$  SD from three independent experiments. Student *t* test was performed and significance levels have been defined as  $p < 0.05$ ; \* $p < 0.001$  vs the corresponding unstimulated rafts

carcinogenesis,<sup>1,36–39</sup> as well as to be involved in tumor progression and in the metastatic cascade.<sup>40</sup> Therefore, since the differential and specific roles of the two splicing variants in carcinogenesis are still controversial, experimental approaches, and new in vitro models, mimicking the tissue organization and the epithelial-stromal interactions occurring in vivo, would represent powerful tools to study in details the contribution of each isoform in the process of tumorigenesis.

In the present study, we have started from our previous findings that, in normal human keratinocytes, the switching from FGFR2b to FGFR2c,<sup>8</sup> or the forced expression of FGFR2c<sup>9</sup> are able to trigger EMT. This switching is induced by down-modulation of the epithelial splicing regulatory proteins 1 and 2 (ESRP1 and ESRP2), which are known to control the alternative splicing events of different genes,<sup>41</sup> including FGFR2.<sup>8,42</sup> Here we analyzed the impact of the FGFR2-mediated EMT process on the stratification and matrix invasion in organotypic skin equivalent rafts and the possible cellular and molecular mechanisms involved. The results obtained indicate that the impairment of basal layer formation of FGFR2c expressing clones, possibly due to the altered actin cytoskeletal organization and to the incapacity to efficiently assemble new junctions, as a consequence of the down-modulation of crucial cell-cell adhesion molecules such as E-cadherin or of desmosomal components such as DSG1, may represent the initial event responsible for the overall defective differentiation and stratification. This impairment in regenerating organotypic epidermis becomes highly evident when the FGFR2c cultures are further stimulated by the ligand FGF2, an effect which is opposite to the enhancement of the differentiation induced by treatment of the clones expressing FGFR2b with the corresponding specific ligand FGF7, and these observations strongly support the hypothesis that receptor switching would be responsible for altering the paracrine response of normal keratinocytes to stromal-derived growth factors and to the microenvironment.

The key role played by the fibroblasts embedded in the dermal equivalent, mimicking the stromal architecture of the human skin, is not only ascribed to their ability to secrete growth factors for the epidermal cells, such as the FGFs, but also to their capacity of remodeling the collagen matrix which, in the context of the carcinogenic process, can promote the invasiveness of epidermal tumor cells.<sup>31,43</sup> Our results are consistent with such role, demonstrating that the invasive potential shown by the normal keratinocytes, when forced to express FGFR2c, required the presence in the gel matrix of the dermal fibroblasts. Because our previous study has demonstrated that this FGFR2c expression in keratinocytes triggers type III EMT and N-cadherin appearance<sup>9</sup> and it has been proposed by others that N-cadherin-mediated cell-cell adhesion induces the collective cell invasion mode in epithelial cells undergoing EMT,<sup>44</sup> future work will be focused on the detailed analysis of the collective or isolated invasive behavior of our FGFR2c keratinocyte model and on the molecular mechanisms regulating the process.

Finally, since we showed that the forced FGFR2c expression is linked to the up-modulation of p63, in agreement with the molecular and functional p63/FGFR interplay which would be unbalanced in SCC

initiation and progression,<sup>15,16</sup> our cell models of FGFR2b or FGFR2c expressing keratinocyte clones will be useful in comparing them with selected human SCC cell lines or primary epithelial tumors characterized by opposite profiles of FGFR2b/2c expression or carrying p63 mutations.

Taken together, our results support the hypothesis that the receptor switching from FGFR2b to FGFR2c and the consequent appearance of the mesenchymal FGFR2c variant in the human epidermal context would drive the early steps of carcinogenesis inducing defective differentiation and stratification as well as invasion of the collagen matrix. This tumorigenic potential might be triggered by the unbalancing of the p63/FGFR interplay and deregulation of the paracrine response of normal keratinocytes to stromal-derived growth factors and to the microenvironment.

## ACKNOWLEDGMENTS

We thank Ms Silvia Caputo for excellent technical assistance. This work was partially supported by grants from MIUR and from AIRC—Associazione Italiana per la Ricerca sul Cancro, Italy. Grant number: IG 15858.

## CONFLICTS OF INTEREST

The authors declare that they have no conflicts of interest.

## ORCID

Maria Rosaria Torrisi  <http://orcid.org/0000-0003-2692-9312>

## REFERENCES

1. Turner N, Grose R. Fibroblast growth factor signalling: from development to cancer. *Nat Rev Cancer*. 2010;10:116–129.
2. Goetz R, Mohammadi M. Exploring mechanisms of FGF signalling through the lens of structural biology. *Nat Rev Mol Cell Biol*. 2013;14:166–180.
3. Petiot A, Conti FJ, Grose R, Revest JM, Hodivala-Dilke KM, Dickson C. A crucial role for Fgfr2-IIIb signalling in epidermal development and hair follicle patterning. *Development*. 2003;130:5493–5501.
4. Grose R, Fantl V, Werner S, et al. The role of fibroblast growth factor receptor 2b in skin homeostasis and cancer development. *EMBO J*. 2007;26:1268–1278.
5. Yang J, Meyer M, Müller AK, et al. Fibroblast growth factor receptors 1 and 2 in keratinocytes control the epidermal barrier and cutaneous homeostasis. *J Cell Biol*. 2010;188:935–952.
6. Belleudi F, Purpura V, Torrisi MR. The receptor tyrosine kinase FGFR2b/KGFR controls early differentiation of human keratinocytes. *PLoS ONE*. 2011;6:e24194.
7. Purpura V, Belleudi F, Caputo S, Torrisi MR. HPV16 E5 and KGFR/FGFR2b interplay in differentiating epithelial cells. *Oncotarget*. 2013;4:192–205.
8. Ranieri D, Belleudi F, Magenta A, Torrisi MR. HPV16 E5 expression induces switching from FGFR2b to FGFR2c and epithelial-mesenchymal transition. *Int J Cancer*. 2015;137:61–72.
9. Ranieri D, Rosato B, Nanni M, Magenta A, Belleudi F, Torrisi MR. Expression of the FGFR2 mesenchymal splicing variant in epithelial cells drives epithelial-mesenchymal transition. *Oncotarget*. 2016;7:5440–5460.

10. Zhao Q, Caballero OL, Davis ID, et al. Tumor-specific isoform switch of the fibroblast growth factor receptor 2 underlies the mesenchymal and malignant phenotypes of clear cell renal cell carcinomas. *Clin Cancer Res*. 2013;19:2460–2460.
11. Oltean S, Sorg BS, Albrecht T, et al. Alternative inclusion of fibroblast growth factor receptor 2 exon IIIc in Dunning prostate tumors reveals unexpected epithelial mesenchymal plasticity. *Proc Natl Acad Sci USA*. 2006;103:14116–14121.
12. Candi E, Cipollone R, Rivetti di Val Cervo P, Gonfloni S, Melino G, Knight R. P63 in epithelial development. *Cell Mol Life Sci*. 2008;65:3126–3133.
13. Truong AB, Kretz M, Ridky TW, Kimmel R, Khavari PA. P63 regulates proliferation and differentiation of developmentally mature keratinocytes. *Genes Dev*. 2006;20:3185–3197.
14. Oh JE, Kim RH, Shin KH, Park NH, Kang MK. DeltaNp63a protein triggers epithelial-mesenchymal transition and confers stem cell properties in normal human keratinocytes. *J Biol Chem*. 2011;286:38757–38767.
15. Ramsey MR, Wilson C, Ory B, et al. FGFR2 signaling underlies p63 oncogenic function in squamous cell carcinoma. *J Clin Invest*. 2013;123:3525–3538.
16. Dotto GP. P63 and FGFR: when development meets proliferation. *EMBO Mol Med*. 2012;4:165–167.
17. Boukamp P, Petrussevska RT, Breitkreutz D, Hornung J, Markham A, Fusenig NE. Normal keratinization in a spontaneously immortalized aneuploid human keratinocyte cell line. *J Cell Biol*. 1988;106:761–771.
18. Raffa S, Leone L, Scrofani C, Monini S, Torrisi MR, Barbara M. Cholesteatoma-associated fibroblasts modulate epithelial growth and differentiation through KGF/FGF7 secretion. *Histochem Cell Biol*. 2012;138:251–269.
19. Anacker D, Moody C. Generation of organotypic raft cultures from primary human keratinocytes. *J Vis Exp*. 2012;60:e3668.
20. Pickard A, Cichon AC, Barry A, et al. Inactivation of Rb in stromal fibroblasts promotes epithelial cell invasion. *EMBO J*. 2012;31:3092–3103.
21. Ye J, Coulouris G, Zaretskaya I, Cutcutache I, Rozen S, Madden TL. Primer-BLAST: a tool to design target-specific primers for polymerase chain reaction. *BMC Bioinformatics*. 2012;13:134.
22. Simpson CL, Patel DM, Green KJ. Deconstructing the skin: cytoarchitectural determinants of epidermal morphogenesis. *Nat Rev Mol Cell Biol*. 2011;12:565–580.
23. Jones MC, Caswell PT, Norman JC. Endocytic recycling pathways: emerging regulators of cell migration. *Curr Opin Cell Biol*. 2006;18:549–557.
24. Capone A, Visco V, Belleudi F, et al. Up-modulation of the expression of functional keratinocyte growth factor receptors induced by high cell density in the human keratinocyte HaCaT cell line. *Cell Growth Differ*. 2000;11:607–614.
25. Getsios S, Simpson CL, Kojima S, et al. Desmoglein 1-dependent suppression of EGFR signaling promotes epidermal differentiation and morphogenesis. *J Cell Biol*. 2009;185:1243–1258.
26. Harmon RM, Simpson CL, Johnson JL, et al. Desmoglein-1/Erbin interaction suppresses ERK activation to support epidermal differentiation. *J Clin Invest*. 2013;123:1556–1570.
27. Shamir ER, Ewald AJ. Three-dimensional organotypic culture: experimental models of mammalian biology and disease. *Nat Rev Mol Cell Biol*. 2014;15:647–664.
28. Pickard A, McDade SS, McFarland M, McCluggage WG, Wheeler CM, McCance DJ. HPV16 down-regulates the insulin-like growth factor binding protein 2 to promote epithelial invasion in organotypic cultures. *PLoS Pathog*. 2015;11:e1004988.
29. Barbaresi S, Cortese MS, Quinn J, Ashrafi GH, Graham SV, Campo MS. Effects of human papillomavirus type 16 E5 deletion mutants on epithelial morphology: functional characterization of each transmembrane domain. *J Gen Virol*. 2010;91:521–530.
30. Barton CE, Johnson KN, Mays DM, et al. Novel p63 target genes involved in paracrine signaling and keratinocyte differentiation. *Cell Death Dis*. 2010;1:e74.
31. Gaggioli C, Hooper S, Hidalgo-Carcedo C, et al. Fibroblast-led collective invasion of carcinoma cells with differing roles for RhoGTPases in leading and following cells. *Nat Cell Biol*. 2007;9:1392–1400.
32. Haugsten EM, Wiedlocha A, Olsnes S, Wesche J. Roles of fibroblast growth factor receptors in carcinogenesis. *Mol Cancer Res*. 2010;8:1439–1452.
33. Brooks AN, Kilgour E, Smith PD. Molecular pathways: fibroblast growth factor signaling: a new therapeutic opportunity in cancer. *Clin Cancer Res*. 2012;18:1855–1862.
34. Feng S, Wang F, Matsubara A, Kan M, McKeehan WL. Fibroblast growth factor receptor 2 limits and receptor 1 accelerates tumorigenicity of prostate epithelial cells. *Cancer Res*. 1997;57:5369–5378.
35. Zhang Y, Wang H, Toratani S, et al. Growth inhibition by keratinocyte growth factor receptor of human salivary adenocarcinoma cells through induction of differentiation and apoptosis. *Proc Natl Acad Sci USA*. 2001;98:11336–11340.
36. Kawase R, Ishiwata T, Matsuda Y, et al. Expression of fibroblast growth factor receptor 2 IIIc in human uterine cervical intraepithelial neoplasia and cervical cancer. *Int J Oncol*. 2010;36:331–340.
37. Matsuda Y, Hagio M, Seya T, Ishiwata T. Fibroblast growth factor receptor 2 IIIc as a therapeutic target for colorectal cancer cells. *Mol Cancer Ther*. 2012;11:2010–2020.
38. Ishiwata T, Matsuda Y, Yamamoto T, Uchida E, Korc M, Naito Z. Enhanced expression of fibroblast growth factor receptor 2 IIIc promotes human pancreatic cancer cell proliferation. *Am J Pathol*. 2012;180:1928–1941.
39. Peng WX, Kudo M, Fujii T, Teduka K, Naito Z. Altered expression of fibroblast growth factor receptor 2 isoform IIIc: relevance to endometrioid adenocarcinoma carcinogenesis and histological differentiation. *Int J Clin Exp Pathol*. 2014;7:1069–1076.
40. Chaffer CL, Brennan JP, Slavin JL, Blick T, Thompson EW, Williams ED. Mesenchymal-to-epithelial transition facilitates bladder cancer metastasis: role of fibroblast growth factor receptor-2. *Cancer Res*. 2006;66:11271–11278.
41. Warzecha CC, Shen S, Xing Y, Carstens RP. The epithelial splicing factors ESRP1 and ESRP2 positively and negatively regulate diverse types of alternative splicing events. *RNA Biol*. 2009;6:546–562.
42. Warzecha CC, Sato TK, Nabet B, Hogenesch JB, Carstens RP. ESRP1 and ESRP2 are epithelial cell-type-specific regulators of FGFR2 splicing. *Mol Cell*. 2009;13:33. 591–601.
43. Izar B, Joyce CE, Goff S, et al. Bidirectional cross talk between patient-derived melanoma and cancer-associated fibroblasts promotes invasion and proliferation. *Pigment Cell Melanoma Res*. 2016;29:656–658.
44. Shih W, Yamada S. N-cadherin-mediated cell-cell adhesion promotes cell migration in a three-dimensional matrix. *J Cell Sci*. 2012;125:3661–3670.

## SUPPORTING INFORMATION

Additional Supporting Information may be found online in the supporting information tab for this article.

**How to cite this article:** Ranieri D, Rosato B, Nanni M, Belleudi F, Torrisi MR. Expression of the FGFR2c mesenchymal splicing variant in human keratinocytes inhibits differentiation and promotes invasion. *Molecular Carcinogenesis*. 2018;57:272–283.

<https://doi.org/10.1002/mc.22754>